# Reaction-diffusion equations on a sphere: Meandering of spiral waves

Jagannathan Gomatam and Faridon Amdjadi
*Department of Mathematics, Glasgow Caledonian University, Cowcaddens Road, Glasgow G4 OBA, United Kingdom*
(Received 23 April 1997; revised manuscript received 16 June 1997)

Numerical integration of an excitable reaction-diffusion (RD) system on a sphere is presented. The evolution of counterrotating double spiral waves on this manifold is studied and it is shown that tips of the spiral can either perform a meandering motion or rigidly rotate around a fixed center, depending on the system control parameter. This transition in dynamics is also illustrated by considering the phase plane of the solutions of the RD system. [S1063-651X(97)03410-7]

PACS number(s): 82.40.Ck, 03.40.Kf, 82.20.Mj, 82.20.Wt

## I. INTRODUCTION

Excitable biological and chemical media support a variety of wave forms of esoteric shapes [1–3], the dominant ones being toroidal scroll waves in three dimensions [4] and spiral or target wave forms on the plane [5]. Winfree [6] pointed out that the spiral wave observed in two-dimensional excitable media, such as the Belousov-Zhabotinsky (BZ) chemical reaction, may not rotate rigidly about a fixed center and that the tip of the spiral wave can perform complex motion. Recently, Barkley, Kness, and Tuckerman [7] simulated a reaction-diffusion (RD) system on the plane and have shown that, depending on the parameters of the system, the spiral wave can execute either a simple (periodic) or compound (quasiperiodic) rotation. They demonstrated that a supercritical Hopf bifurcation is responsible for this transition. In a subsequent paper Barkley [8] considered the RD equations as a two-parameter bifurcation system and studied the interaction between imaginary eigenvalues arising from the symmetry of the plane with Hopf bifurcation eigenvalues; he showed that the point where these eigenvalues coalesce on the path of Hopf bifurcations is the point of emergence of the path of modulated traveling-wave solutions that separate the region of the two kinds of modulated rotating-wave solutions. He obtained some comprehensive results for the RD system on the plane.

Our interest is to consider spiral waves on nonplanar surfaces. The main motivation for studying this type of solution lies in its applicability to problems [1,2] in physiology, biology, and chemistry. Maselko and Showalter [9] performed experiments with the BZ chemical waves propagating on the surface of a sphere. They observed that a spiral wave winds outward from a meandering source at the north pole and undergoes self-annihilation as it winds into itself at the south pole.

The eikonal approximation to the RD system was used by Grindrod and Gomatam [10] to obtain a symmetric counterrotating double spiral wave on the sphere, while McQuillan and Gomatam [5] demonstrated the existence of a class of asymmetric solutions of similar type.

In this work we consider a reaction-diffusion system on a sphere and by numerical integration of the equations we illustrate the formation of a counterrotating double spiral wave, where one of the spiral arms winds out towards the north pole and curls around the pole, while the other arm of the spiral moves towards the south pole and curls back towards the equator. Considering numerical solutions of the system, we demonstrate that, depending on one of the system parameters, the motion can consist of either meandering or rigid rotation around a fixed center. An important feature of our methodology is the introduction of the phase plane for the norms $\|u\|^2=\int_0^{2\pi}|u(\theta,\phi)|^2 d\phi$ and $\|v\|^2=\int_0^{2\pi}|v(\theta,\phi)|^2 d\phi$ at $\theta=\pi/4$; variables $u$ and $v$ are defined in the next section. This approach obviates the need for precise definition of the spiral tip in investigating the qualitative changes in the dynamics of the RD system.

## II. SETTING THE SYSTEM

Consider the reaction-diffusion system of the form

$$\frac{\partial u}{\partial t}=\Delta^2 u+f(u,v), \quad \frac{\partial v}{\partial t}=g(u,v), \tag{1}$$

where $u=u(\theta,\phi,t)$ and $v=v(\theta,\phi,t)$ are defined on a spherical domain with a fixed radius $r$ where $0\leqslant\theta\leqslant\pi$, $0\leqslant\phi\leqslant 2\pi$, and

$$\Delta^2 u=\frac{1}{r^2\sin\theta}\frac{\partial}{\partial\theta}\left(\sin\theta\,\frac{\partial u}{\partial\theta}\right)+\frac{1}{r^2\sin^2\theta}\frac{\partial^2 u}{\partial\phi^2}.$$

The periodicity conditions

$$u(\theta,0)=u(\theta,2\pi)\quad\forall t, \quad v(\theta,0)=u(\theta,2\pi)\quad\forall t$$

are inherent in the problem; however, the condition on $v$ is not implemented in the numerical process. The local reaction kinetics are given by

$$f(u,v)=\frac{1}{\epsilon}u(1-u)(u-u_{\rm th}), \quad g(u,v)=u-v,$$

where $u_{\rm th}=(v+b)/a$ and $a$, $b$, and $\epsilon\ll 1$ are the system parameters. This kinetics is used by Barkley, Kness, and Tuckerman [7] in the study of the periodic-quasiperiodic transition for the planar spiral waves. The variables $u$ and $v$ are known as the excitation and the recovery variables, respectively.

The system is singular at $\theta=0$ and $\pi$. This singularity can be dealt with as follows. (i) Assume that, near the poles, the variable $u$ is symmetrical with respect to the poles; therefore,

 

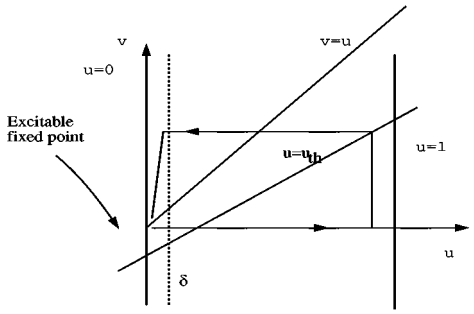


FIG. 1. Local reaction kinetics. Steady states of the system are defined by Eq. (2). An excitable fixed point is located at the origin; $u_{\mathrm{th}}$ is the excitability threshold. Subthreshold perturbations (initial excitations on the left-hand side of the threshold) result in a simple return to the origin, while superthreshold perturbations (initial excitations on the right-hand side of the threshold) result in trajectories that sweep the state towards some new (excited) regime, before returning (perhaps via a prolonged cycle of behavior) to the rest point. $\delta$ denotes a small boundary layer; the system spends most of the time within this region.

at these points, the term $(1/\tan\theta)(\partial u/\partial\theta)$ can be approximated by $\partial^2 u/\partial\theta^2$. (ii) Since the point $(0,\phi)$ for all $0\leqslant\phi\leqslant 2\pi$ defines the north pole, we require

$$u(0,\phi)=u(0,\phi+\alpha)\quad \forall\,\alpha\in\mathbb{R};$$

otherwise $u=u(0,\phi)$ is not a single-valued function of $\phi$. This condition implies that $u=u(0,\phi)$ is a constant function of $\phi$, i.e., $u_{\phi\phi}=0$; this implies that the term $(1/\sin^2\theta)(\partial^2 u/\partial\phi^2)$ can be omitted at the north pole. A similar argument applies for $\theta=\pi$. Thus at $\theta=0$ and $\pi$, the system takes the form

$$\frac{\partial u}{\partial t}=\frac{2}{r^2}\frac{\partial^2 u}{\partial\theta^2}+f(u,v),\quad \frac{\partial v}{\partial t}=g(u,v).$$

In the absence of the diffusion term, the system has a stable but excitable fixed point at $u=v=0$ (see Fig. 1), which is one of the solutions of the steady-state system defined by

$$f(u,v)=0,\quad g(u,v)=0. \tag{2}$$

Any numerical scheme for solving Eq. (1) must take advantage of the two distinct dynamical states $u$ and $v$. To be precise, consider a small boundary layer $\delta$ near the left branch of $u$ shown in Fig. 1. We call a given point in the spatial domain excited if $(u,v)$ lies outside the boundary layer, i.e., if $u>\delta$. A point in the spatial domain is recovered if it is within the boundary layer.

### III. NUMERICAL SIMULATION

At any instant of the time, almost all the spatial points are within a small boundary layer (see Fig. 2). This figure shows that only at the excited part of the wave $u\neq 0$; otherwise $u=0$. Therefore, the reaction term can be time stepped efficiently with little effort. Thus we time step the kinetics by means of the following algorithm [11]. If $u^n<\delta$, then

$$u^{n+1}=0,\quad v^{n+1}=(1-\Delta t)v^n;$$

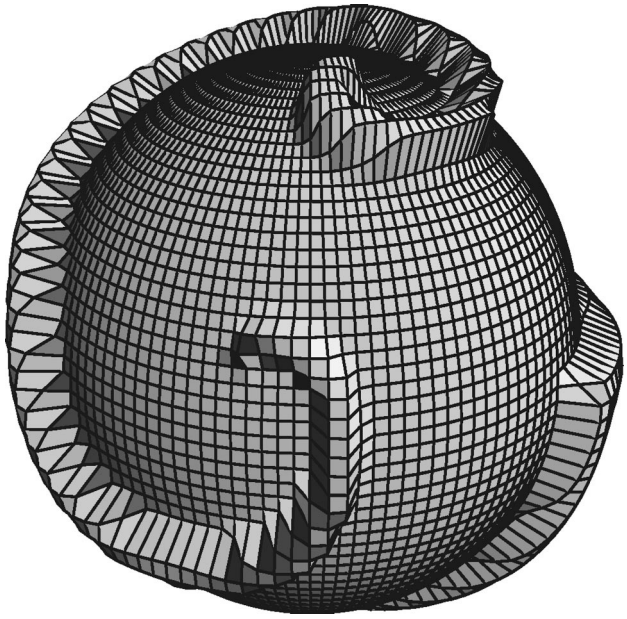

FIG. 2. Meandering of the spiral wave on the sphere. The parameters are $\Delta t=1.0/1500.0$, $t=9.0$, $N_\theta=61$, $N_\phi=120$, $r=16.0$, $a=0.35$, and $b=0.0008$.

otherwise

$$u_{\mathrm{th}}=\frac{v^n+b}{a},$$

$$v^{n+1}=v^n+\Delta t(u^n-v^n), \tag{3}$$

$$u^{n+1}=u^n+(\Delta t/\epsilon)u^n(1-u^n)(u^n-v_{\mathrm{th}}),$$

where $u^n$ and $v^n$ are the values of the $u$ and the $v$ variables at the $n$th time step (at some point in the spatial domain), $\Delta t$ is the time step, and $\delta$ is the size of a small boundary layer, where the points on the left of this boundary directly tend to the origin. Using this algorithm implies that within the boundary layer kinetic terms require only one conditional evaluation and one floating-point multiplication.

We simulate Eq. (1) as follows. The surface of the sphere is discretized with $N_\phi=120$ in the $\phi$ direction and $N_\theta=61$ in the $\theta$ direction. We denote $u(\theta,\phi)$, at the grid point $(i,j)$ and the $n$th time step, as $u_{ij}^n$. Therefore, the second derivative is approximated by the fourth-order finite-difference formula [12]

$$\left(\frac{\partial^2 u}{\partial\theta^2}\right)_{i,j}=\frac{1}{h^2}\left(\delta_\theta^2 u_{ij}^n-\tfrac{1}{12}\delta_\theta^4 u_{ij}^n\right)+O(h^4):=F_{i,j}+O(h^4),$$

$$\left(\frac{\partial^2 u}{\partial\phi^2}\right)_{i,j}=\frac{1}{k^2}\left(\delta_\phi^2 u_{ij}^n-\tfrac{1}{12}\delta_\phi^4 u_{ij}^n\right)+O(k^4):=T_{i,j}+O(k^4),$$

where $\delta_\theta u_{i,j}=u_{i+1/2,j}^n-u_{i-1/2,j}^n$, $\delta_\phi u_{i,j}=u_{i,j+1/2}^n-u_{i,j-1/2}^n$, and $h$ and $k$ are grid sizes in the $\theta$ and $\phi$ directions, respectively. The first-order derivatives are evaluated by second-order central finite differences and the reaction term time stepped by algorithm (3). With these finite-difference formulas the Laplacian takes the form

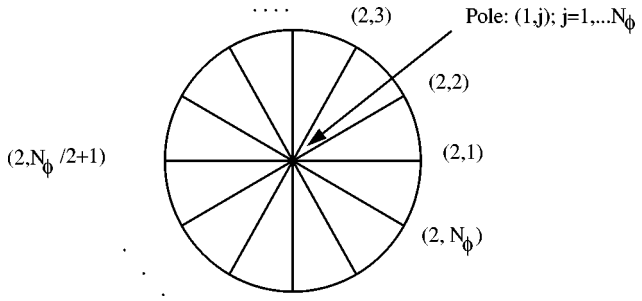


FIG. 3. Discretization around the north pole.

$$\Delta^2 u = \frac{1}{r^2 \tan\theta_i}(\Delta_\theta u_{i,j} + \nabla_\theta u_{i,j}) + O(h^2) + F_{i,j} + O(h^4) + \frac{1}{r^2 \sin^2\theta_i} T_{i,j} + O(k^4),$$

where $\theta_i = (i-1)h$ and $i = 2, \ldots, N_\theta - 1$; $j = 1, \ldots, N_\phi$. Obviously, the truncation error for this approximation excluding the poles is $O(k^4) + O(h^2)$. At the poles, say, the north pole,

$$\Delta^2 u = \frac{2}{r^2 h^2}\left[\tfrac{-1}{12}(u_{3,1} + u_{-1,1}) + \tfrac{4}{3}(u_{2,1} + u_{0,1}) - \tfrac{5}{2}u_{1,1}\right] + O(h^4).$$

The truncation error at the poles is $O(h^4)$. Note that the terms $u_{0,1}$ and $u_{-1,1}$ are not in the range of discretization. The layout of grids near the poles, say, the north pole, is shown in Fig. 3. Therefore, the use of central difference approximation for $\partial u/\partial\theta$ at this pole implies

$$\left(\frac{\partial u}{\partial \theta}\right)_{1,1} = \frac{1}{2h}(u_{2,1} - u_{2,(N_\phi/2)+1}).$$

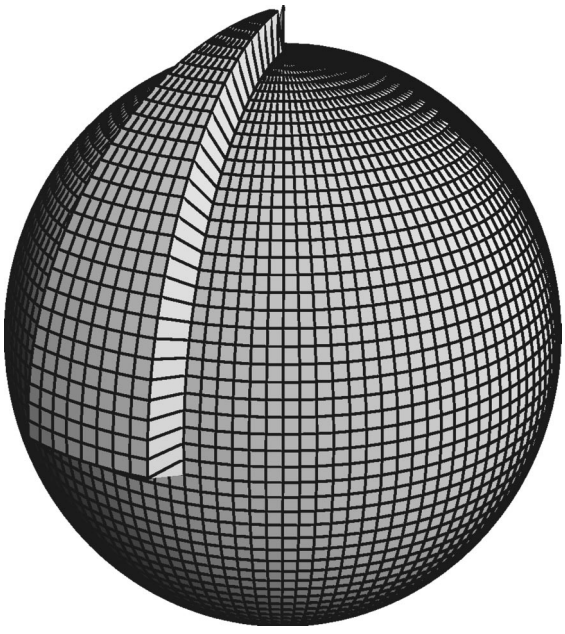

FIG. 4. Initial solution at $t = 0$.

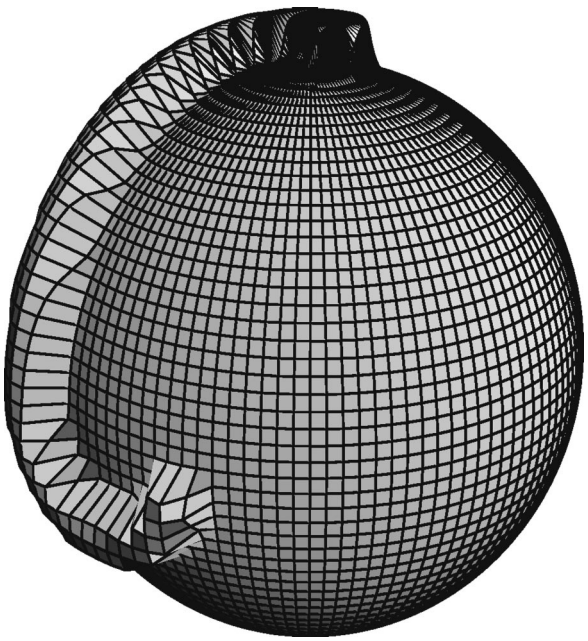

FIG. 5. Formation of the spiral wave at $t = 1$.

On the other hand, using the central difference approximation formula with $i = 1$ and $j = 1$ implies

$$\left(\frac{\partial u}{\partial \theta}\right)_{1,1} = \frac{1}{2h}(u_{2,1} - u_{0,1}).$$

Thus $u_{0,1} = u_{2,(N_\phi/2)+1}$. A similar argument implies $u_{-1,1} = u_{3,(N_\phi/2)+1}$.

There are only three system parameters $a$, $b$, and $\epsilon$ by which the properties of the medium can be adjusted and four numerical parameters $\delta$, $\Delta t$, $h$, and $k$, where we choose $h \approx k$. The radius of the sphere whose surface is the domain of excitation is also important in our simulation. For a small

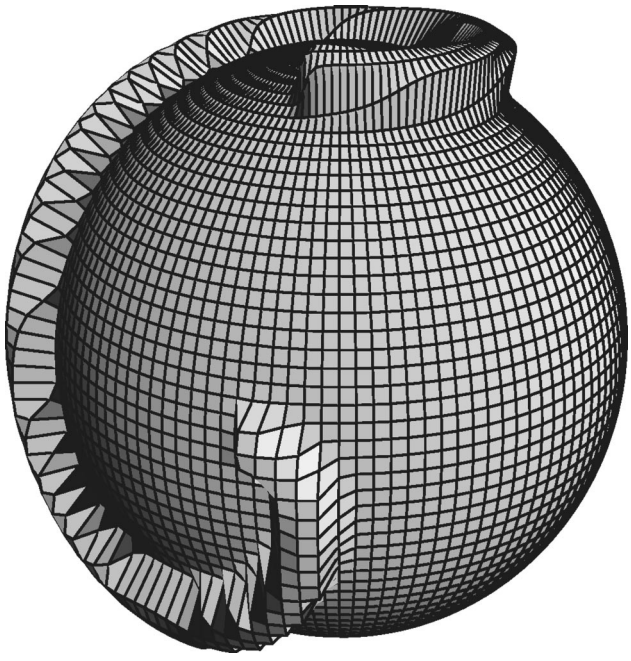

FIG. 6. Formation of the spiral wave at $t = 2$.

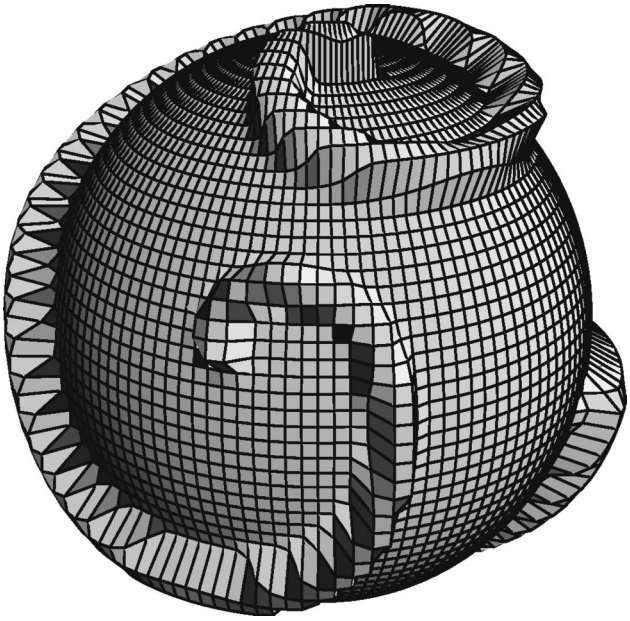

FIG. 7. Meandering of the spiral wave on the sphere. The parameters are $\Delta t = 1.0/1500.0$, $t = 9.5$, $N_\theta = 61$, $N_\phi = 120$, $r = 16.0$, $a = 0.35$, and $b = 0.0008$.

radius the spiral wave may never be excited and for a large radius the time step must be decreased significantly, which is computationally expensive and may also cause numerical instabilities. We considered that for this problem $r \in [11,16]$ is the reasonable regime where the wave can be excited. However, we choose $r = 16.0$ in order to allow enough domain of excitation for the spiral wave to perform a complete rotation.

Initially, it is natural to set both variables $u$ and $v$ to nonzero values at some points in the spatial domain. Thus we start our simulation with the excitation variable $u = 0.9$ closer to the right branch of the steady state $u = 1.0$ along a thin strip from the north pole to the equator (see Fig. 4). We set $v = 0.6$ from the north pole to the equator on the immediate left- (or right-) hand side of the $u$ excitation. Setting these nonzero values for the recovery variable $v$ on one side of the $u$ excitation has the following merits: (i) It prevents the annihilation of the wave propagation, at the starting period of times, by requiring that this part of the sphere is in a recovery period and (ii) it prevents the propagation towards the west (east).

The initial excitations in the fast variable $u$ and the slow

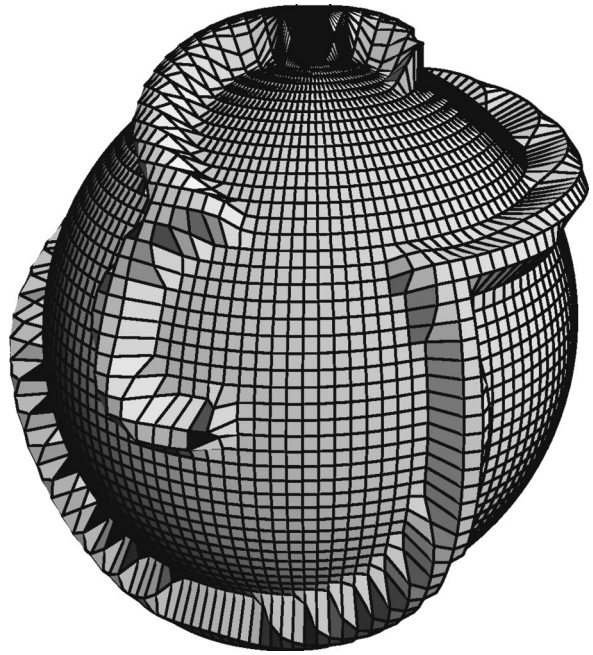

FIG. 9. Meandering of the spiral wave on the sphere. The parameters are $\Delta t = 1.0/1500.0$, $t = 10.5$, $N_\theta = 61$, $N_\phi = 120$, $r = 16.0$, $a = 0.35$, and $b = 0.0008$.

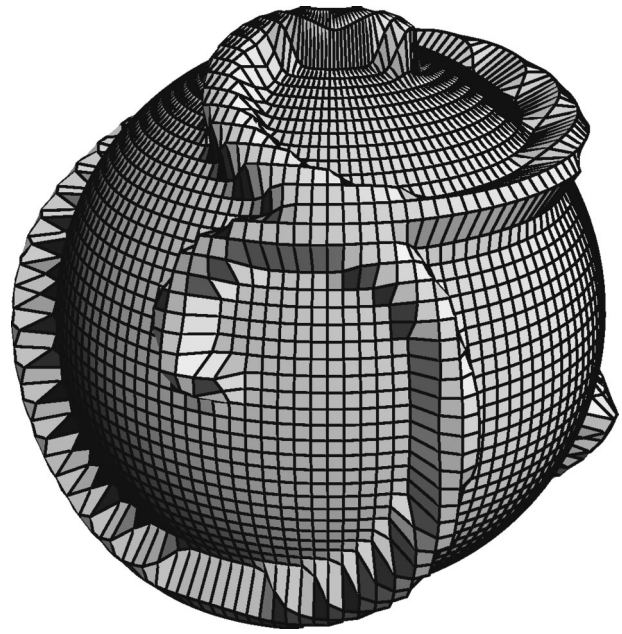

FIG. 8. Meandering of the spiral wave on the sphere. The parameters are $\Delta t = 1.0/1500.0$, $t = 10.0$, $N_\theta = 61$, $N_\phi = 120$, $r = 16.0$, $a = 0.35$, and $b = 0.0008$.

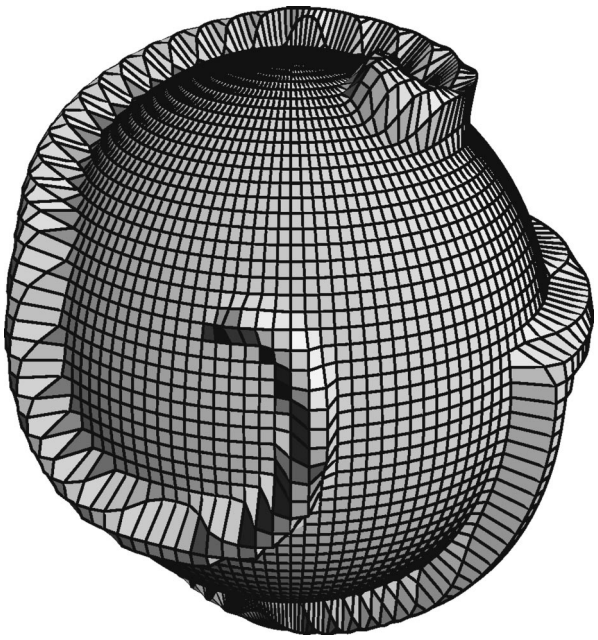

FIG. 10. Meandering of the spiral wave on the sphere. The parameters are $\Delta t = 1.0/1500.0$, $t = 12.0$, $N_\theta = 61$, $N_\phi = 120$, $r = 16.0$, $a = 0.35$, and $b = 0.0008$.

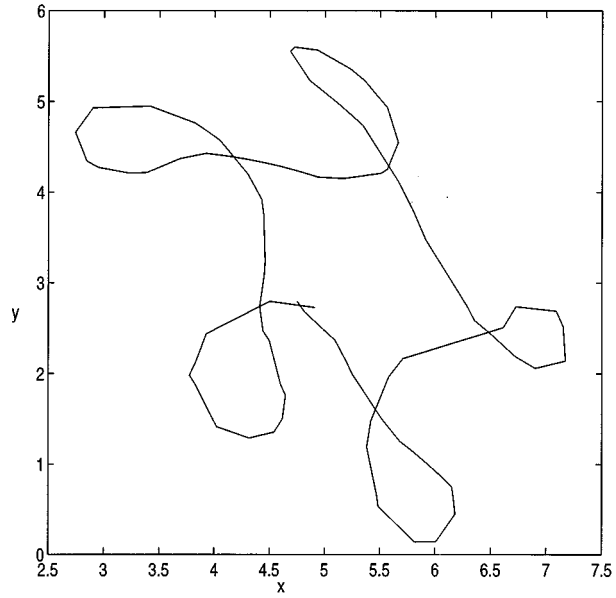


FIG. 11. Spiral tip path rotation. The spiral tip path is taken by five complete rotations; $N_\theta = 131$, $N_\phi = 260$, $a = 0.35$, and $b = 0.0008$.

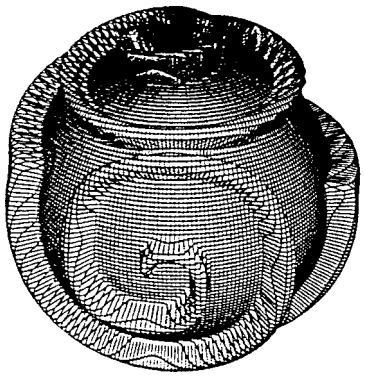

FIG. 12. Meandering of the spiral wave on the sphere. The parameters are $\Delta t = 1.0/10\,000.0$, $t = 10.0$, $N_\theta = 131$, $N_\phi = 260$, $r = 29.0$, $a = 0.35$, and $b = 0.0008$.

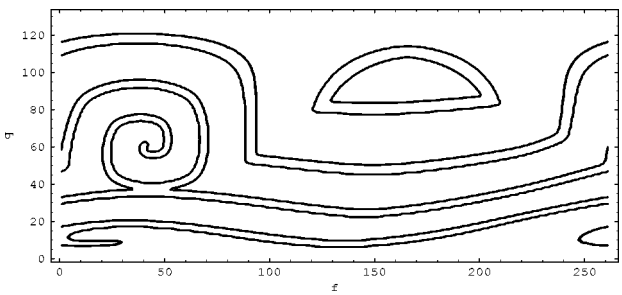


FIG. 13. Contour plot of the fast variable $u$. $0 \leqslant \theta \leqslant \pi$, $0 \leqslant \phi \leqslant 2\pi$, $N_\theta = 131$, $N_\phi = 260$, $u = 0.3$, 0.4.

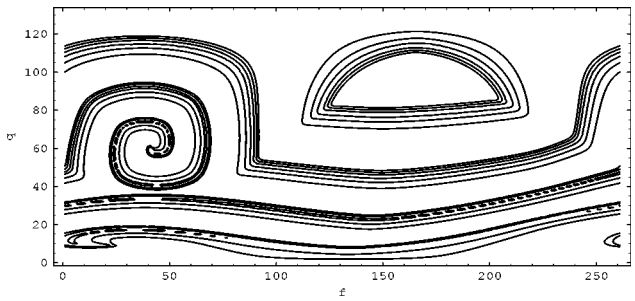


FIG. 14. Contour plot of the slow variable $v$. $0 \leqslant \theta \leqslant \pi$, $0 \leqslant \phi \leqslant 2\pi$, $N_\theta = 131$, $N_\phi = 260$, $v = 0.1$, 0.2, 0.3, 0.4, 0.5.

variable $v$ are sufficient, via the diffusion in the excitation variable $u$, to instigate a propagating spiral wave. Therefore, with these initial values, the variable $u$ dominates the behavior of the system and a spiral wave starts propagating. At the beginning of the evolution process (see Figs. 5 and 6), the spiral tip at the north pole rotates to the left and the wave emerges at the front of the sphere, while the other end of the spiral moves towards the south pole and curls back towards the equator; this gives rise to a counterrotating double spiral on the sphere. As time evolves, two different segments of the same wave front collide and the wave front splits into two parts (see Figs. 8 and 9): The large loop undergoes self-annihilation near the south pole, while the short remaining part of the wave gives rise to a new generation of the spiral wave (see Fig. 10). This process of the spiral wave rotation continues on the sphere as time progresses. One complete rotation is given by Figs. 2 and 7–10; these graphs show that a spiral wave at, say, $t = 9.0$ returns to the same position after some period of time at $t = 12.0$. Our numerical results are in agreement with the experimentally obtained waves reported by Maselko and Showalter [9].

As the wave rotates on the sphere the shape of the spiral changes near the tips of the spiral. Because our spatial do-

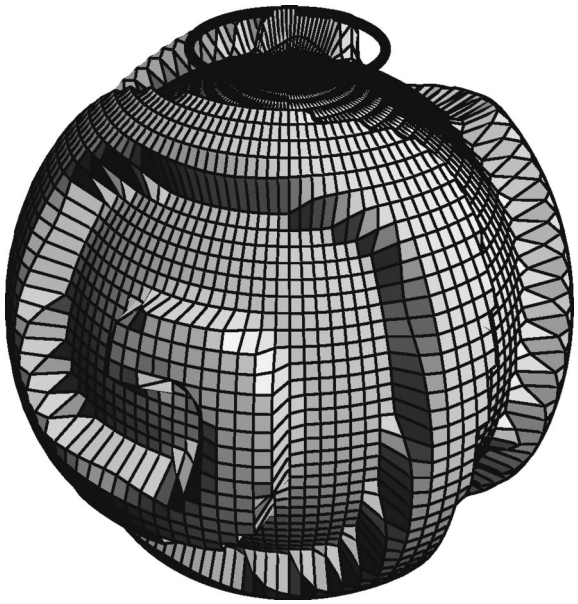

FIG. 15. Rigid rotation of the spiral wave on the sphere. The parameters are $\Delta t = 1.0/1500.0$, $t = 5.0$, $N_\theta = 61$, $N_\phi = 120$, $r = 16.0$, $a = 0.85$, and $b = 0.0008$.

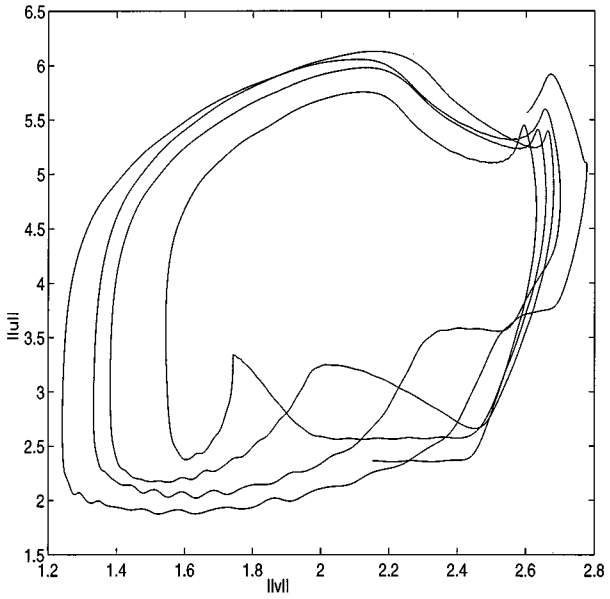


FIG. 16. Transition from rigid rotation to meandering motion. The parameter $a=0.4$.

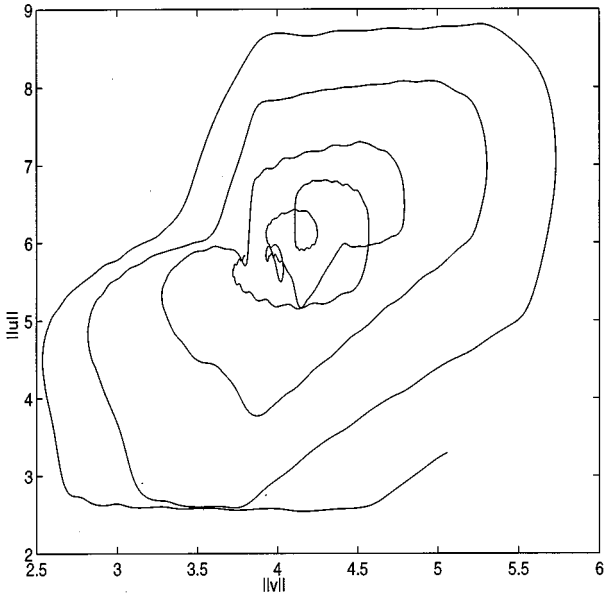


FIG. 18. Transition from rigid rotation to meandering motion. The parameter $a=0.75$.

main is without boundaries, the wave has the freedom to propagate in two different directions with two tips. We have demonstrated that for some parameter values, the spiral tips follow the meandering trajectories. Thus the spiral wave rotation for these parameters is the compound rotation. Figure 11 shows a path taken by one of the spiral tips (the tip at southern hemisphere) during five complete rotations for some parameter values. The motion of the spiral tip is conveniently studied by projecting the instantaneous state of the system onto the $x$-$y$ plane. We take the spiral tip to be the intersection of the two contours $u=0.5$ and $f(0.5,v)=0$. This definition [7] of the spiral tip enables us to find it among numerical solutions. However, identifying the spiral tip needs a fine discretization. The spiral tips in Figs. 2 and 7–10 exhibit complex motion, but with the discretization reported above, it is not possible to obtain quantitative results on this motion. The spiral tip path shown in Fig. 11 is given with $N_\theta=131$ and $N_\phi=260$. Figure 12 shows spiral waves with these grids and a significantly smaller time step. Contour plots with this resolution for the excitation variable $u$ and the recovery variable $v$ are given in Figs. 13 and 14.

The qualititative aspect of the dynamics depends on the control parameter $a$. As this parameter varies between 0.35 and 0.95 we observe that some transition occurs around $a=0.80$. For $a=0.85$ the spiral wave, after a very short time interval, rotates rigidly around a fixed center and the two spiral tips rotate accordingly; the tip at the southern hemisphere traces out a fixed point on the $x$-$y$ plane and is nearly stationary, while the tip at the northern hemisphere rotates around the axis of the sphere, i.e., a core around the north

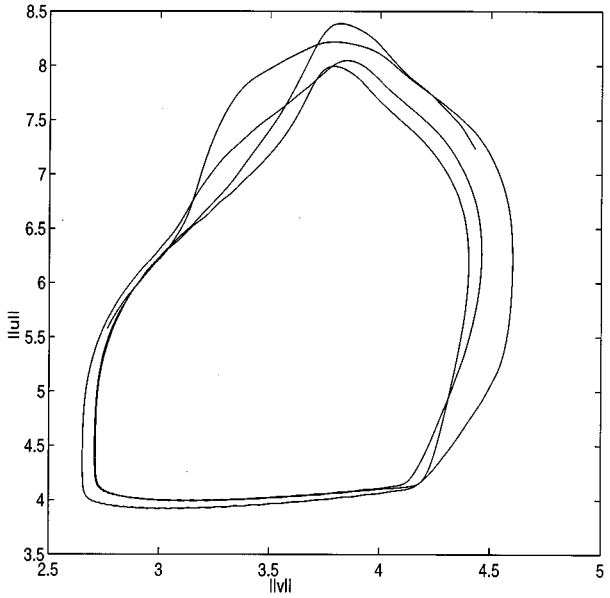


FIG. 17. Transition from rigid rotation to meandering motion. The parameter $a=0.65$.

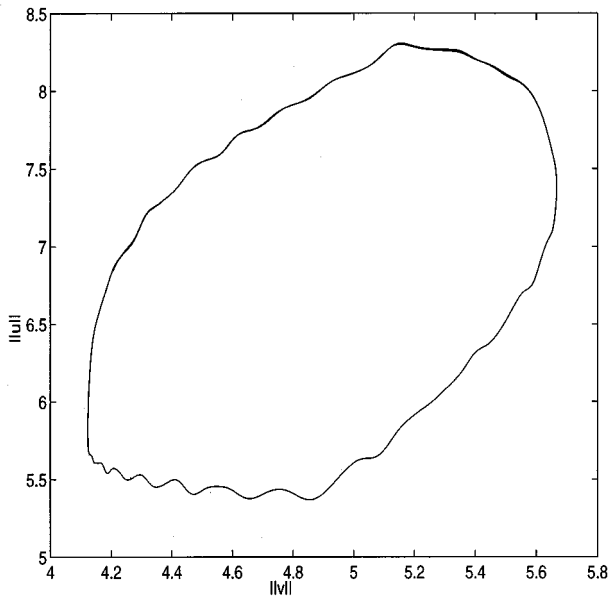


FIG. 19. Transition from rigid rotation to meandering motion. The parameter $a=0.85$.

pole. Figure 15 shows a simple rotation of the spiral wave in which the circle on the north pole is the path taken by the spiral tip. Considering the full solution set $(u,v)$ of the coupled system, it is easier and computationally inexpensive to explore the qualitative changes of the dynamics. Figures 16–19 show a sequence of solution states obtained as a function of the parameter $a$.

The time-dependent simulation of the RD system can elucidate qualitative properties of the wave evolution as illustrated in Figs. 16–19. A comprehensive understanding of theexcitable media on nonplanar surfaces, including the transition from a rigid rotation to meandering motion, is possible only with a bifurcation analysis of the RD system; this problem will be considered elsewhere.

## IV. CONCLUSION

In the present work, by starting with random initial values for the excitation and the recovery variables $u$ and $v$, respectively, and by adjusting some system parameter, we demonstrate the existence of a counterrotating double spiral wave with their tips propagating in two different directions as time evolves. The spiral tips can trace out either meandering motion or rotate around a fixed center as evident in the projection of their motion on the $x$-$y$ plane, depending on the system control parameter $a$. We have also shown that the transition from simple to complex rotation can be obtained by considering the numerical solution of the coupled system and studying the phase plane of $\|u\|$ and $\|v\|$. The motion of the spiral wave studied in this paper is in qualititative agreement with the experimental observation of Maselko and Showalter [9].

Finally, we observed that the rotation of the wave on spherical surface is similar to that obtained by Barkley, Kness, and Tuckerman [7] on the planar surface, except that in the absence of the boundary on a spherical surface some parts of the wave undergo self-annihilation in contrast to the spiral wave behavior on bounded planar surfaces.

## ACKNOWLEDGMENT

The authors wish to thank A.J. Mulholland for the useful discussion and hints on surface waves.

[1] A. T. Winfree, *When Time Breaks Down* (Princeton University Press, Princeton, 1987).
[2] J. D. Murrey, *Mathematical Biology* (Springer-Verlag, New York, 1989).
[3] B. J. Welsh, J. Gomatam, and A. E. Burgess, Nature (London) **304**, 611 (1983).
[4] B. J. Welsh and J. Gomatam, Physica D **43**, 304 (1990).
[5] P. McQuillan and J. Gomatam, J. Phys. Chem. **100**, 5157 (1996).
[6] A. T. Winfree, Science **181**, 353 (1973).
[7] D. Barkley, M. Kness, and L. S. Tuckerman, Phys. Rev. A **42**, 2489 (1990).
[8] D. Barkley, Phys. Rev. Lett. **72**, 164 (1994).
[9] J. Maselko and K. Showalter, Nature (London) **339**, 609 (1989).
[10] P. Grindrod and J. Gomatam, J. Math. Biol. **25**, 597 (1987).
[11] D. Barkley, J. Phys. D **49**, 61 (1991).
[12] G. D. Smith, *Numerical Solution of Partial Differential Equations* (Clarendon, Oxford, 1985).